

## OPTIMIZE PRODUCTION THROUGH RESERVOIR ROCK COMPACTION CONTROL

ARIFFIN SAMSURI<sup>1</sup> & PHAM VU CHUONG<sup>2</sup>

**Abstract.** This paper presents compactional laboratory study based on the various controllable parameters such as wellbore angle, perforation shot density, perforation pattern, and flow rate to determine the effects of these parameters to compaction in order to help optimize production through compaction control. The study was conducted on local sandstone core sample. After the mechanical rock properties were determined, the scaled down models with various borehole angles, perforation shot densities, perforation patterns and flow rates were tested with Servo Controlled Compression Testing Machine (SCCTM) using two techniques; static and dynamic tests. The results show that compaction increases as borehole angle, production flow rate and shot density increase and as perforation pattern changes from spiral to inplane and finally inline. In addition, compaction increases slowly at low effective stress. However when effective stress reaches 30-60% of reservoir rock compressive strength, it increases approximately double and followed by the reduction of total oil recovery to 55-73% of the expected total oil recovery. These results show that it is possible to optimize production rate via minimizing compaction which could be achieved by controlling borehole angle, perforation shot density, perforation pattern, and flow rate.

*Key Words:* Rock compaction, compressive strength, shot density, perforation pattern, wellbore angle

### 1.0 INTRODUCTION

Most of oil and gas wells produce through sandstone formation that are deposited in marine or detritus environments. Marine deposits are often cemented with calcareous or siliceous minerals and may be strongly consolidated. In contrast, Miocene and younger sands are often unconsolidated or poorly consolidated with soft clay or silt. During the production of oil and gas, the pore fluid pressure would generally decline and thus increase effective stress within the reservoir. Increasing of the effective stress acting on the contact between grain to grain in the unconsolidated or poorly consolidated sandstone will permit the rock compact easily.

In general, reservoir rock compaction is the process that always has adverse effects on the oil and gas wells such as well production reduction, casing

<sup>1&2</sup> Faculty of Chemical and Natural Resources Engineering, Universiti Teknologi Malaysia, 81310 Skudai, Johor Darul Ta'zim.

collapse, and land subsidence. It is one of the major problems in many petroleum fields throughout the world, and has become subject of research for many years. In 1973, Geertsma *et al.* [1] performed a field, experimental, and mathematical studies to examine the land subsidence of oil and gas fields, particularly at the Groningen gas field in Netherland. They recognized three individual parameters that influenced reservoir rock compaction as well as land subsidence. There were reduction of reservoir pressure, vertical extents of the zone in which pore pressure reduction has taken place, and order of magnitude of the relevant deformation property of the reservoir rock. They also concluded that subsidence was a results of reservoir compaction which in turn relied on the product of reservoir pressure reduction, height of productive interval, and rock compressibility. Through an experimental study of rock properties change during reservoir compaction, Morita *et al.* [2] concluded that during reservoir rock compaction, rock properties could be characterized by three stages, namely the initial non-linear portion where grain contact points opened and closed with small stress change, followed by the linear portion where stable structure deformed linearly, and finally the non-linear portion where microcracks grew before failure. In addition, Johnson and Rhett [3] presented a study based on laboratory tests and concluded that Ekofisk chalk furnished elastic and pore collapse deformation of the high porosity chalk accounts for the majority of reservoir compaction.

By using an axisymmetric Finite Element Method, Chia and Bradley [4] simulated rock compaction and casing deformation in reservoir along the Gulf Coast, which were overpressured and undercompacted. They concluded that the depletion of an underconsolidated and overpressured reservoir might result in severe rock compaction. It was not only within sand reservoir but also in adjacent clay or shale formation hence contributed to casing deformation. Generally a large increase in casing stress and strain usually occurs during the early stage of production as a result of rapid pressure decline in the vicinity of the wellbore.

Based on physical and finite element modelling, Ariffin [5] concluded that the perforated wellbore might undergo compaction before failure which generally depends on pressure differential, perforation length, perforation diameter, model geometry, and rock properties. General, reservoir rock compaction is mainly influenced by pore fluid pressure depletion, depending on completion and production activities. For perforated completion, the pressure reduction increases as the perforation length, perforation diameter, shot density, and underbalanced pressure increase. During production, rapid pore pressure depletion occurs at higher amount of flow rate and produced fluid [6]. Furthermore, completion and production processes also cause reduction of reservoir rock strength hence contribute to compaction.

General  
to reduc  
In addit  
which re  
that con  
stress, re  
wellbore  
density,  
reservoir  
be exam  
suitable  
problem  
effects of  
rate to co

## 2.0 EX

### 2.1 San

Two type  
low poros  
7.0 millid  
high porc  
dynamic  
compressi  
were trim  
samples v  
borehole c

### 2.2 Unia

In this te  
connected  
to the Hoe  
of the SC  
(ASTM s  
deformati  
displaceme  
strength (C  
using the f

Generally, completion and production activities will increase compaction due to reduction of reservoir rock strength and elevation of pore pressure depletion. In addition, the dominant effect of compaction is the reduction of porosity which result in decreasing of well productivity [7]. Previous works have shown that compaction was affected by both uncontrollable parameters such as rock stress, rock strength, and pore pressure and controllable parameters such as wellbore structure, perforation length, perforation diameter, perforation shot density, and flow rate. In planning for the production of oil and gas from a reservoir, if compaction is foreseen, however, controllable parameters need to be examined carefully in order to control reservoir rock compaction. The suitable completion design method need to be selected to minimize this problem as well as to optimize the production. This study aims to analyze the effects of wellbore angle, perforation shot density, perforation pattern, and flow rate to compaction to help optimize production through compaction control.

## 2.0 EXPERIMENTAL

### 2.1 Sample Preparation

Two types of local sandstone core samples were used in this study. One with low porosity, ranging from 7.0 to 13.0% and permeability ranging from 3.0 to 7.0 millidarcy (md) was used for static compaction test and another one with high porosity (15.0 to 17.0%) and permeability (25 to 100md) was used for dynamic compaction test. These core samples were prepared for uniaxial compression and compaction tests. For uniaxial compression tests, samples were trimmed to cylindrical shape of 5.08 cm × 12.7 cm. For compaction test, samples were trimmed to cylindrical model of 15.24 cm × 15.24 cm, with borehole of 5.08 cm diameter and cemented casing of 2.54cm diameter.

### 2.2 Uniaxial Compression Tests

In this test, the specimen was placed inside the rubber sleeve, which was connected to the Hoek Cell. The axial and radial strain gauges were connected to the Hoek Cell. The whole assembly was placed centrally within the platens of the SCCTM, then load was applied at a constant rate of 0.7 MN/m<sup>2</sup>/sec (ASTM standard) until the specimen fails. The process of specimen deformation could be monitored from the computer. The axial, radial displacement, and axial load were recorded. Then uniaxial compressive strength ( $C_o$ ), Young modulus ( $E$ ), and Poisson's ratio ( $\nu$ ) were calculated by using the following equations [8,9]:

$$C_o = \frac{F}{A} \quad (1)$$

$$E = \frac{\sigma_z}{\varepsilon_z} \quad (2)$$

$$\nu = -\frac{\varepsilon_y}{\varepsilon_z} \quad (3)$$

### 2.3 Compaction Tests

Compaction tests were carried out under two conditions namely static and dynamic. Static compaction test was performed on models with different borehole angles of 0, 5, 10, 15 and 20°, different perforation shot densities of 4, 6, 8 and 16 shot per foot (SPF) and different perforation patterns of inline, inplane, and spiral. Dynamic compaction test was performed on models with different flow rates of 400, 800, and 1600 ml/h.

### 2.4 Static Compaction Tests

Considering a gradient of overburden pressure 6.43 kPa (1 psi/ft) and pore pressure 2.89 kPa (0.45 psi/ft), for the sample at depth of 3658 m (12 000 feet), the 77.14 MPa (12 000 psi) of overburden, and 36 MPa (5600 psi) of confining pressures were modelled. The testing was designed to keep overburden load constant and reduce confining pressure until the model fail. Models with different wellbore angles, perforation shot densities, and patterns were put centrally under the SCCTM. After overburden and confining pressures were increased to 77.14 MPa (12 000 psi) and 36 MPa (5600 psi), respectively, the confining pressure was reduced at a constant rate of 100 KPa/s until the model fails. The axial displacement was recorded from the computer. Then compaction degree was calculated using Equations (4) and (5):

$$C_m = \left( \frac{1 + \nu}{1 - \nu} \right) \left( \frac{1 - 2\nu}{E} \right) \quad (4)$$

$$\frac{\Delta h}{h} = C_m * \Delta P_f \quad (5)$$

### 2.5 Dynamic Compaction Test

It was designed to maintain the confining pressure and increase overburden load until the model fails. Models were put centrally under the SCCTM. Initially confining pressure was increased to 1.5 MPa with a constant rate of 100 KPa/s. Then pore pressure was increased to 1.35 MPa with a constant rate of 100 KPa/s to simulate flow rate of 400 ml/h for drawdown of 1.25 MPa with 60 cp oil. After flow rate stabilised, the axial load was increased with a constant rate of 0.7 MN/m<sup>2</sup> until the model fails. The axial displacement was recorded from the computer and then compaction degree was calculated using Equation (4).

Repeat the w  
simulate flow

### 3.0 RESULT

Results of unia  
to low to me  
Poisson's ratio  
in compaction

Sample Gro
Medium stren
Low strength

Generally, c  
density, perfor  
angle, shot der  
from spiral to

### 3.1 Effect of

Summarized r  
shown in Tabl  
compaction de  
the compaction  
0.00065, 0.000  
shows that the  
increases. The  
compressive str  
failed at 93.5%  
that as the bor  
and result in  
Therefore com

It is because,  
hole and the pr  
concluded that  
slide along the  
greatest. Theref

(2)

Repeat the whole procedure with pore pressures of 3.5 MPa and 6 MPa to simulate flow rates of 800 ml/h and 1600 ml/h respectively with 60 cp oil.

(3)

### 3.0 RESULTS AND DISCUSSIONS

Results of uniaxial tests are shown in Table 1. These sandstone samples belong to low to medium strength (according to Deere and Miller, 1969). The Poisson's ratio from this test was used to calculate the coefficient of compaction in compaction tests using Equation (4).

**Table 1** Results of uniaxial compression tests

Sample Group	Compressive strength (MPa)	Young modulus (GPa)	Poisson ratio
Medium strength	67.5	15.02	0.16
Low strength	21.0	7.60	0.32

Generally, compaction is influenced by borehole angle, perforation shot density, perforation pattern, and flow rate. Compaction increases as borehole angle, shot density, and flow rate increase and as perforation pattern changes from spiral to inplane and inline.

#### 3.1 Effect of Borehole Angle

Summarized results of compaction tests with different borehole angles are shown in Table 2. Figure 1 shows that for a 4 SPF and inline pattern, the compaction degree of the vertical borehole at break or failure is 0.00062. While the compaction at break for 5°, 10°, 15°, and 20° borehole angle models were 0.00065, 0.00084, 0.00087, and 0.00091 respectively. In addition, Figure 1 also shows that the compaction degree decreases as the pore pressure depletion increases. The vertical model failed after effective stress reaches 94.7% of compressive strength. While the 5°, 10°, 15°, and 20° borehole angle models failed at 93.5%, 90.5%, 88.2% and 80.6%, respectively. These results show that as the borehole angle increases, the rock is found to be more easier to fail and result in more compaction depending on the pore pressure depletion. Therefore compaction can be minimized through allowable borehole angle.

It is because, an inclined borehole creates angular relationship between borehole and the principal stress axes hence increases the shear stress. Thus, it can be concluded that as the wellbore angle increases, there is a tendency to shear or slide along the borehole inclination since the concentration of the shear stress is greatest. Therefore, compaction increases as the borehole angle increases.

(4)

(5)

ely, static and  
with different  
hot densities of  
terns of inline,  
on models with

si/ft) and pore  
n (12 000 feet),  
si) of confining  
verburden load  
. Models with  
terns were put  
pressures were  
respectively, the  
in the model  
puter. Then

verburden load  
DTM. Initially  
of 100 KPa/s.  
of 100 KPa/s  
60 cp oil. After  
ate of 0.7 MN/  
ded from the  
Equation (4).

**Table 2** Summarized results of compaction tests with different borehole angles

Pore pressure depletion (MPa)	Compaction degree				
	0°	5°	10°	15°	20°
0	0.00000	0.00000	0.00000	0.00000	0.00000
11	0.00000	0.00000	0.00000	0.00000	0.00003
14	0.00000	0.00002	0.00005	0.00002	0.00005
17	0.00000	0.00006	0.00008	0.00006	0.00008
20	0.00002	0.00009	0.00011	0.00013	0.00013
23	0.00004	0.00013	0.00015	0.00017	0.00025
26	0.00015	0.00023	0.00024	0.00026	0.00034
29	0.00021	0.00028	0.00033	0.00036	0.00043
31	0.00034	0.00038	0.00042	0.00050	0.00053
32	0.00043	0.00040	0.00047	0.00057	0.00061
33	0.00047	0.00048	0.00052	0.00065	0.00070
34	0.00048	0.00053	0.00062	0.00071	0.00091
35	0.00062	0.00065	0.00085	0.00087	-

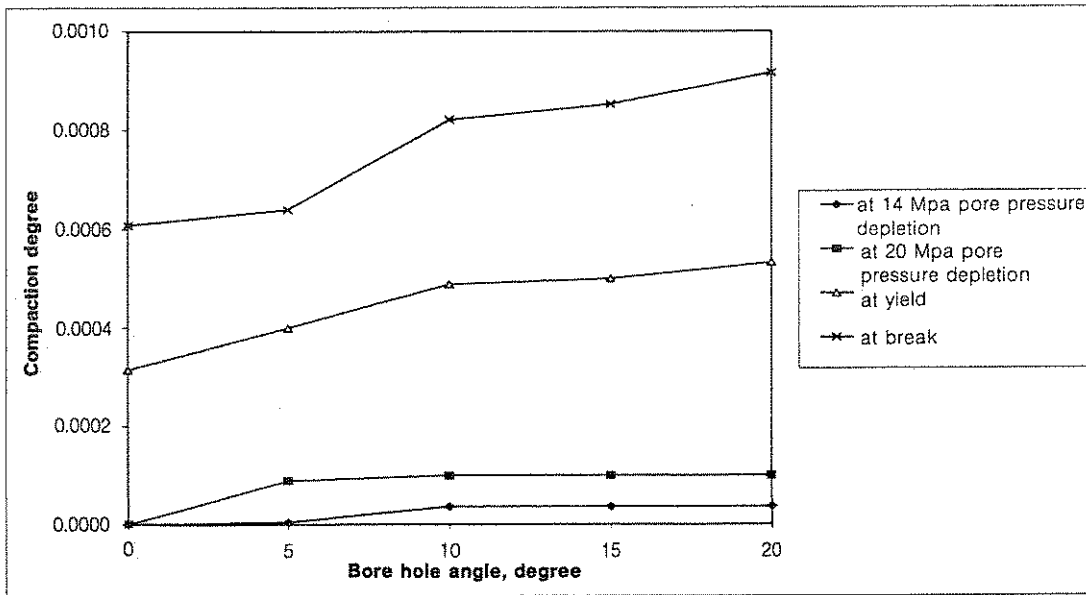


**Figure 1** Effects of bore hole angle to compaction

**3.2 Effects**

Summarized are shown in compaction i borehole and break or failu of model with also shows the increases. The by 93.8%, 84 results show t result in mc Therefore, m important cor This pheno critical drawd very high den carry more re rock mass str

**Table 3** Sumi

Pore pressure depletion (MPa)
0
0
14
17
20
23
26
29
31
32
33
34
35

### 3.2 Effects of Perforation Shot Density

Summarized results of compaction tests with different perforation shot densities are shown in Table 3. Figure 2 shows that as pore pressure depleted, compaction increases depending on perforation shot density. For a vertical borehole and inline pattern, the compaction degree of model with 4 SPF at break or failure is 0.00062 compared to 0.00081 of model with 6 SPF, 0.00095 of model with 8 SPF, and 0.00096 of model with 16 SPF. In addition, Figure 2 also shows that the compaction degree decreases as the pore pressure depletion increases. The 4 SPF model fails at 94.68% of compressive strength, followed by 93.8%, 84.3%, and 70.9% for 6, 8, and 16 SPF models, respectively. These results show that as shot density increases, the model will be easier to fail and result in more compaction depending on the pore pressure depletion. Therefore, minimize shot density for acceptable compaction degree is an important consideration during the well design stage.

This phenomenon occurs due to the fact that as shot density increases, the critical drawdown for shear failure decreases due to stress relief, especially for very high density. In addition, as shot density increases, the rock mass has to carry more redistributed stress along the perforation system. As a result, the rock mass strength is reduced significantly as shot density increases. Since

**Table 3** Summarized results of compaction tests with different perforation shot densities

Pore pressure depletion (MPa)	Compaction degree			
	4 SPF	6 SPF	8 SPF	16 SPF
0	0.00000	0.00000	0.00000	0.00000
14	0.00000	0.00000	0.00000	0.00007
17	0.00000	0.00002	0.00006	0.00011
20	0.00002	0.00006	0.00010	0.00019
23	0.00004	0.00008	0.00014	0.00024
26	0.00015	0.00020	0.00023	0.00034
29	0.00021	0.00028	0.00033	0.00042
31	0.00034	0.00033	0.00039	0.00063
32	0.00043	0.00034	0.00051	0.00096
33	0.00047	0.00043	0.00060	-
34	0.00048	0.00053	0.00095	-
35	0.00062	0.00081	-	-

borehole angles

20°
0.00000
0.00003
0.00005
0.00008
0.00013
0.00025
0.00034
0.00043
0.00053
0.00061
0.00070
0.00091
-

14 Mpa pore pressure depletion
20 Mpa pore pressure depletion
yield
break

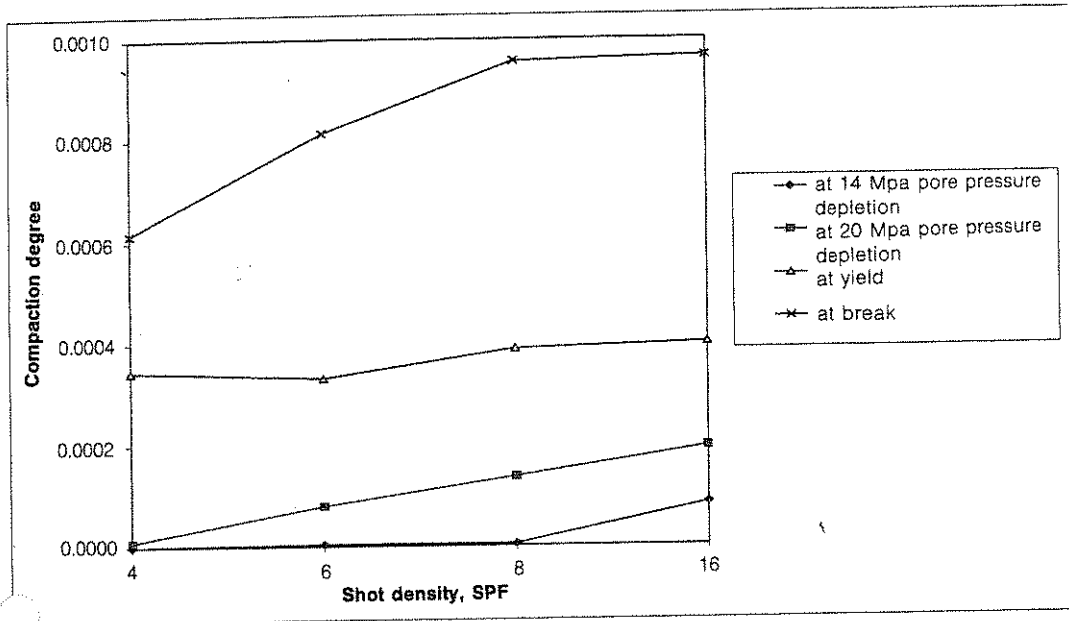


Figure 2 Effects of shot density to compaction

compaction increases as rock strength decreases, therefore compaction degree will increase as shot density increases.

### 3.3 Effects of Perforation Pattern

Summarized results of compaction tests with different perforation patterns are shown in Table 4. Figure 3 shows the effects of perforation pattern to compaction. As pore pressure depleted, compaction increases. However the increment is influenced by perforation pattern of the model. For vertical borehole with 16 SPF, the model with spiral perforation pattern has least compaction at break (0.00080). The compaction of model with inplane perforation pattern at break is 0.00085. Finally model with inline perforation pattern has the most compaction (0.00096). In addition, Figure 3 also shows that the compaction degree decreases as the pore pressure depletion increases. The 16 SPF and spiral model failed at 92.3% of compressive strength, while the inplane and inline models failed at 87.5% and 70.9%, respectively. These results show that as perforation pattern changes from spiral to inplane and finally inline, compaction increases.

The phenomenon is understandable since the perforation tunnels in the inline pattern are in one vertical line, which is parallel to the applied load and provide the shortest distance between perforation holes. Thus resulting in lower rock mass stress than for inplane pattern where the perforation tunnels are in one horizontal line, which is perpendicular to the applied load. Therefore, rock

Table 4 Su

Pore pressure depletion (M)
0
14
17
20
23
26
29
31
32
33
34
35

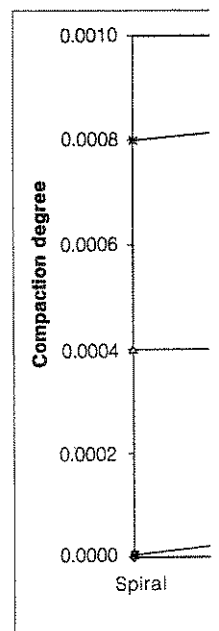




**Table 4** Summarized results of compaction tests with different perforation patterns

Pore pressure depletion (MPa)	Compaction degree		
	Inline	Inplane	Spiral
0	0.00000	0.00000	0.00000
14	0.00007	0.00000	0.00000
17	0.00011	0.00000	0.00002
20	0.00019	0.00001	0.00003
23	0.00024	0.00005	0.00004
26	0.00034	0.00010	0.00007
29	0.00042	0.00022	0.00010
31	0.00063	0.00030	0.00025
32	0.00096	0.00031	0.00030
33	—	0.00041	0.00039
34	—	0.00050	0.00044
35	—	0.00085	0.00080

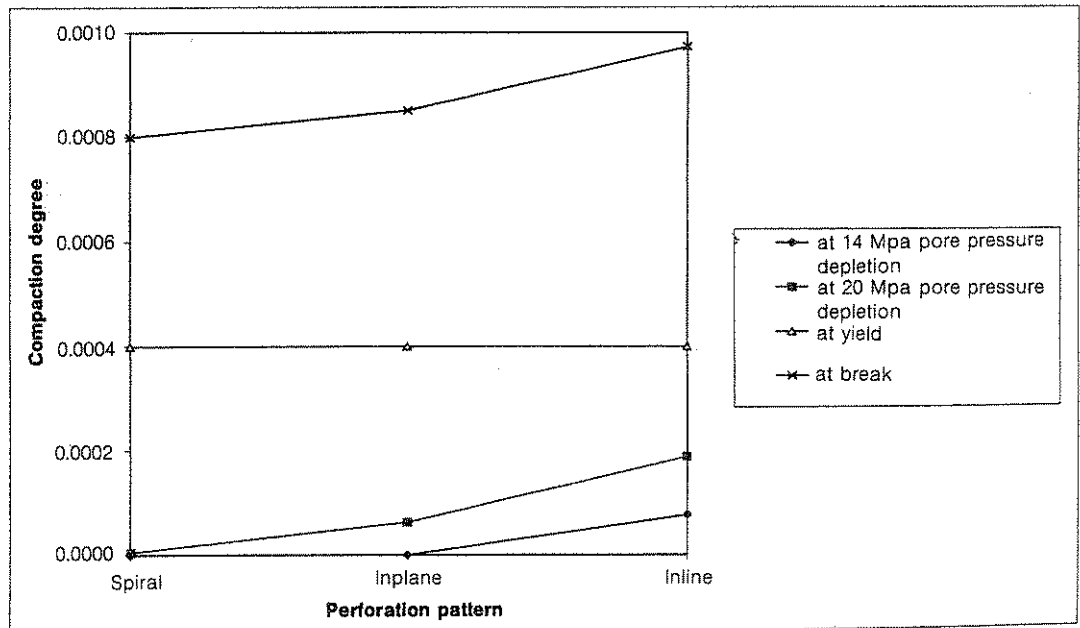


**Figure 3** Effects of perforation pattern to compaction

ore pressure  
ore pressure



tion degree

patterns are  
pattern to  
lower the  
For vertical  
rn has least  
with inplane  
perforation  
3 also shows  
on increases.  
length, while  
ively. These  
inplane and

nnels in the  
ied load and  
ting in lower  
nnels are in  
erefore, rock

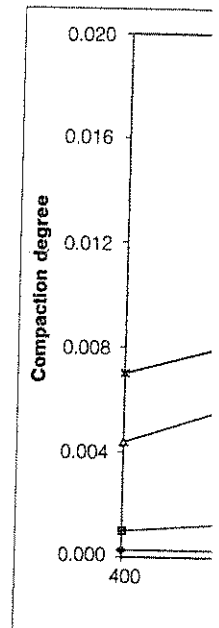
mass stress in an inplane pattern is higher than in an inline pattern. As for the spiral pattern, the perforation tunnels are in a plane inclined to the applied stress resulting in higher rock mass stress than for two previous patterns. The spiral pattern also produces the greatest distance between each successive perforation and therefore the strongest perforated structure. Therefore compaction is highest for the inline pattern, followed by an inplane and finally spiral pattern, since compaction and sand production increase as the rock mass strength decreases, especially the inline pattern.

### 3.4 Effects of Flow Rate

Summarized results of compaction tests with different flow rates are shown in Table 5. Figure 4 shows the effects of flow rate to compaction. We can see that as pore pressure depleted, compaction increases depending on flow rate. The

**Table 5** Summarized results of compaction tests with different flow rates

400 ml/h		890 ml/h		1600 ml/h	
Axial stress, MPa	Compaction Degree	Axial stress, Mpa	Compaction degree	Axial stress, MPa	Compaction degree
0.00	0.0000	0.00	0.0000	0.00	0.0000
1.57	0.0001	1.00	0.0002	0.00	0.0000
4.40	0.0006	3.15	0.0006	0.70	0.0000
7.22	0.0009	5.97	0.0011	3.47	0.0005
10.05	0.0015	8.80	0.0017	6.30	0.0007
12.87	0.0019	11.62	0.0023	9.12	0.0018
15.70	0.0022	14.45	0.0025	11.95	0.0028
18.52	0.0025	17.27	0.0028	14.77	0.0032
21.35	0.0030	20.10	0.0035	17.60	0.0037
24.17	0.0044	22.92	0.0041	20.42	0.0045
27.00	0.0050	25.75	0.0064	23.25	0.0050
29.26	0.0069	28.57	0.0078	26.07	0.0055
-	-	31.19	0.0095	28.90	0.0079
-	-	-	-	31.72	0.0091
-	-	-	-	34.55	0.0096
-	-	-	-	37.37	0.0119
-	-	-	-	39.3500	0.0143



model with fl  
with flow rate  
degree, respec  
degree decrea  
rate model fa  
66.29% for 80  
that as flow ra  
the increase o  
acceptable flo

These result  
from a sands  
between wellb  
grain have res  
change unsta  
increases, the  
hence contribu

**3.5 Effects of**  
Effect of comp  
as compaction

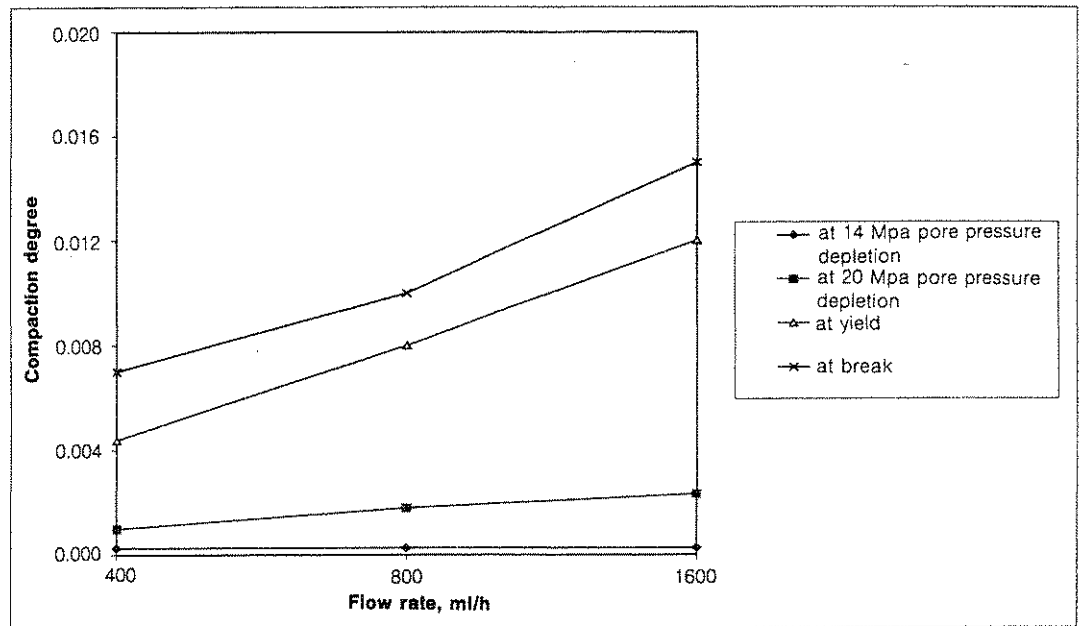


Figure 4 Effects of flow rate to compaction

model with flow rate of 400 ml/h compacted at 0.0069 degree, while model with flow rate of 800 ml/h and 1600 ml/h compacted at 0.0095 and 0.0143 degree, respectively. In addition, Figure 4 also shows that the compaction degree decreases as the pore pressure depletion increases. The 400 ml/h flow rate model failed at 73.7% of compressive strength, followed by 67.1% and 66.29% for 800 ml/h and 1600 ml/h models, respectively. These results show that as flow rate increases, the sandstone model is easier to fail and resulting in the increase of compaction. Therefore, it is possible to control compaction by acceptable flow rate.

These results can be explained by considering that when fluids are produced from a sandstone reservoir, the stress that caused by pressure difference between wellbore and reservoir, and frictional forces that are acting on sand grain have resulted stress state change in the sand formation. Such stress state change unstabilizes the formation and perforation hole. As the flow rate increases, these stresses increase and resulting in grain slipping and sliding hence contribute to compaction.

### 3.5 Effects of Compaction to Produced Oil

Effect of compaction on produced oil is shown in Figure 5. It can be seen that as compaction increases, oil flow rate decreases. Initially, compaction increases

1. As for the the applied attens. The h successive . Therefore inplane and rease as the

are shown in : can see that ow rate. The

v rates

ml/h
0.0000
0.0000
0.0000
0.0005
0.0007
0.0018
0.0028
0.0032
0.0037
0.0045
0.0050
0.0055
0.0079
0.0091
0.0096
0.0119
0.0143

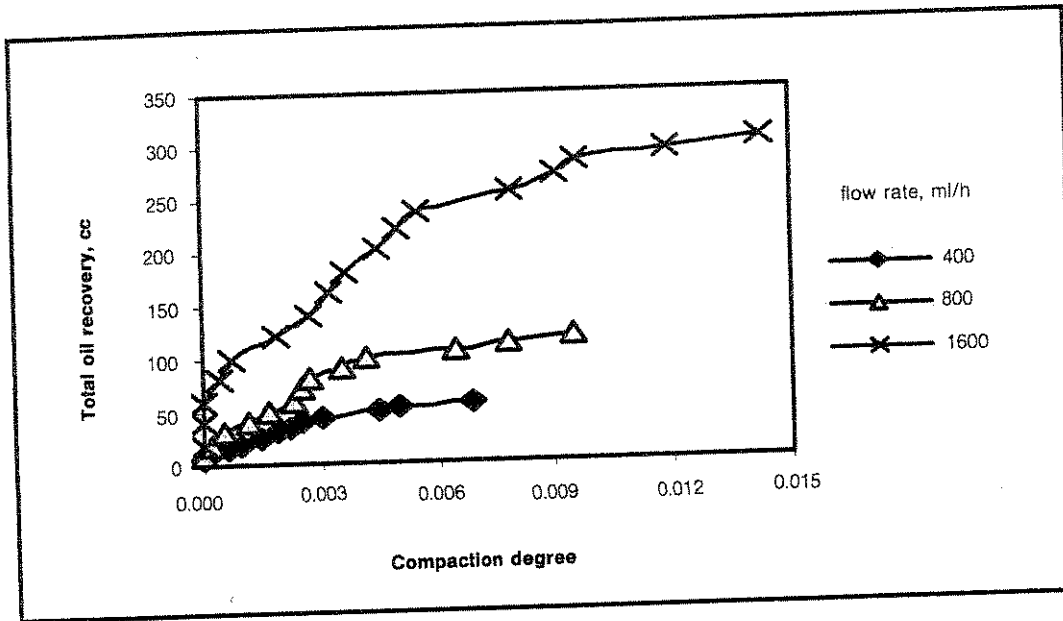


Figure 5 Effects of compaction on total oil recovery

slowly as oil production is stable. However, when compaction degree increases from 0.003 to 0.005 (30-60% of rock compressive strength), the oil production starts to decrease. After sample yield completely and failed, total oil recovery decreases to only 55-73% of the expected oil recovery. It can be explained by the fact that compaction is the process that causes the reduction of porosity and permeability [2,8], therefore flow rate is reduced since flow rate is influenced mainly by porosity and permeability of the reservoir rock.

#### 4.0 CONCLUSIONS

From these experiments, it can be concluded that compaction increases as borehole angle, perforation shot density, and flow rate increase, and as perforation pattern changes from spiral to inplane and inline. The produced oil from the reservoir is influenced by the compaction degree. Oil production starts to decrease significantly after compaction degree reaches 0.003 to 0.004 degree (30-60% of rock compressive strength).

Through understand the effects of borehole angle, perforation shot density, perforation pattern, and flow rate to compaction degree as well as the effects of compaction to flow rate in the designing phase of petroleum well development is very important since production can be optimized via minimizing compaction, which could be achieved by reducing borehole angle, perforation shot density, flow rate, and allowable perforation pattern.

#### NOME

$A$	=
$C_o$	=
$C_m$	=
$E$	=
$F$	=
$\frac{\Delta h}{h}$	=
$\frac{\Delta P_f}{\sigma}$	=
$\sigma$	=
$\epsilon$	=
$u$	=

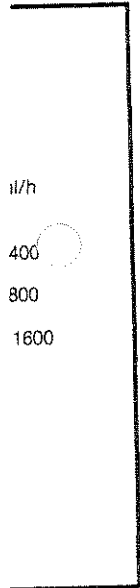
- [1] Ge
- [2] Mc
- [3] Joh
- [4] Chi
- [5] Ari
- [6] Mc
- [7] Lu
- [8] Fja
- [9] Vu

**NOMENCLATURE**

$A$	=	area of cross section, $m^2$
$C_o$	=	compressive strength, MPa
$C_m$	=	coefficient of uniaxial compaction
$E$	=	Young modulus, GPa
$F$	=	force, kN
$\frac{\Delta h}{h}$	=	compaction degree
$\Delta P_f$	=	pore pressure depletion, MPa
$\sigma$	=	stress, MPa
$\epsilon$	=	strain
$\nu$	=	Poisson's ratio

**REFERENCES**

- [1] Geertsma, *et al.* 1973. Land subsidence above compacting of oil and gas reservoir. *Journal of Petroleum Technology*. (June) 734-744.
- [2] Morita, N. *et al.* 1984. *Rock property change during reservoir compaction*. Paper SPE 13099 presented at the SPE 59th Annual Technical Conference and Exhibition held in Houston, Texas, US, September, 16-19.
- [3] Johnson, J.P and D.W. Rhett. 1986. *Compaction behavior of Ekofisk chalk as a function of stress*. Paper SPE 15872 presented at the SPE European Petroleum Conference held in London, UK, October, 221-231.
- [4] Chia, Y. and D. Bradley. 1989. Evaluation of reservoir compaction and its effects on casing behavior. *SPE Production Engineering*. (May): 167-172.
- [5] Ariffin, S. 1990. A study of perforation stability by physical and numerical modeling. PhD theses. University of Strathclyde.
- [6] Morita, N. *et al.* 1989. A quick method to determine subsidence, reservoir compaction and In-situ stress induced by reservoir depletion. *Journal of Petroleum Technology*. (January): 71-79.
- [7] Lundegard, L. 1992. Sandstone porosity loss: a Big-picture view of the important of compaction. *Journal of Sedimentary Petrology*. (March) 250-260.
- [8] Fjaer, E. *et al.* 1992. *Petroleum related rock mechanics*. Amsterdam-London-New York-Tokyo: Elsevier.
- [9] Vutukuri, V. *et al.* 1974. *Handbook on mechanical properties of rocks testing techniques and results*. Trans Tech Publications.



increases  
reduction  
l recovery  
lained by  
ro and  
nfluenced

increases as  
e, and as  
duced oil  
roduction  
3 to 0.004

ot density,  
e effects of  
velopment  
minimizing  
perforation